PHYSICAL REVIEW B **81**, 140503(R) (2010)

Enhanced flux pinning and critical current density via incorporation of self-assembled rare-earth barium tantalate nanocolumns within $YBa_2Cu_3O_{7-\delta}$ films

Sung Hun Wee,[1,2] Amit Goyal,[1] Eliot D. Specht,[1] Claudia Cantoni,[1] Yuri L. Zuev,[1,3] V. Selvamanickam,[4] and Sy Cook[1]
[1]*Materials Science and Technology Division, Oak Ridge National Laboratory, Oak Ridge, Tennessee 37831, USA*
[2]*Department of Materials Science and Engineering, University of Tennessee, Knoxville, Tennessee 37996, USA*
[3]*Department of Physics, University of Tennessee, Knoxville, Tennessee 37996, USA*
[4]*Department of Mechanical Engineering, University of Houston, Houston, Texas 77204, USA*
(Received 14 December 2009; published 16 April 2010)

We report rare-earth barium tantalates, Ba_2RETaO_6 (BRETO, *RE*=rare earth elements) as promising pinning additives for superior flux pinning in $YBa_2Cu_3O_{7-\delta}$ (YBCO) films. BRETO compounds have excellent chemical inertness to and large lattice mismatch with YBCO. This results in phase separation and strain minimization driven self-assembly of BRETO nanocolumns within YBCO films. YBCO+4 vol % Ba_2GdTaO_6 films show similar T_c to that of an undoped film of ~88.3 K, a higher self-field J_c of 3.8 MA/cm^2 at 77 K, and improved in-field J_c higher by a factor of 1.5–6 over entire magnetic field and angular ranges.

DOI: 10.1103/PhysRevB.81.140503 PACS number(s): 74.72.−h, 74.78.Na, 62.23.Pq, 74.25.Sv

Improvement in flux-pinning and consequently critical current density, J_c, in wide magnetic field and angular range is a determining factor in the use of second generation high-temperature superconducting wires for broad range of electric-power applications.[1] In order to realize such improvements in flux-pinning, research efforts have particularly focused on introduction of additional nanoscale defects with several viable and practical methods[2–7] because these defects can immobilize or pin magnetic-flux lines the motion of which reduces J_c. Among the defect structures reported in these studies, the formation of strong *c*-axis correlated columnar defects comprised of self-assembled $BaZrO_3$ (BZO) and $BaSnO_3$ nanodots into $YBa_2Cu_3O_{7-\delta}$ (YBCO) films has proven to be very effective in enhancing pinning over a broad angular regime but particularly for magnetic field parallel to the *c*-axis, $H \| c$.[7–12]

The key driving force for alignment of such BZO nanodots into columns oriented along the *c* axis is the minimization of the misfit strain arising from the lattice mismatch of BZO with YBCO. In other words, a certain minimum level of misfit strain provides the necessary driving force for self-assembly to occur. We have recently found that lattice mismatches in the range of 5–12 % generates adequate misfit strains required for the self-assembly.[13] The experimental and simulation results showed that mismatches below this range do not result in enough misfit strains and hence no *c*-axis-oriented self-assembly occurs and instead, the formation of randomly oriented, epitaxial nanoparticles (for example, in the case of CeO_2 and RE_2O_3) is favored. At very large mismatches above the range, formation of nonepitaxial, random-oriented nanoparticles such as $BaCeO_3$ in YBCO matrix is observed.[13] This study suggested oxide materials within this mismatch range which could potentially be used as additives resulting in better flux-pinning performance than those already reported.

In this Rapid Communication, we introduce rare-earth barium tantalates, Ba_2RETaO_6, (BRETO, *RE*=rare earth elements including Y) as promising additives for strong flux pinning in $REBa_2Cu_3O_{7-\delta}$ superconducting films. BRETO are a group of ordered double perovskites with cubic or distorted cubic cells depending on RE^{3+} ionic radius.[14] Due to their excellent chemical inertness[15] and high lattice mismatch in the range of 9–12 % with YBCO, BRETO additions in YBCO films produced robust columnar defects comprised of self-aligned BRETO nanodots and resulted in strong flux pinning and consequently, massive improvement in J_c over entire field and angular ranges.

The YBCO films with BRETO additions with *RE*=Gd, Er, and Yb were epitaxially grown by pulsed laser deposition using a KrF (λ=248 nm) excimer laser. Laser energy density, repetition rate, and substrate to target distance were 2 J/cm^2, 10 Hz, and 5 cm, respectively. The film growth temperature, T_s, was 1063 K and the oxygen partial pressure, $P(O_2)$, was 230 mTorr. All depositions were performed on ion beam assisted deposition (IBAD)-MgO templates with a $LaMnO_3$ cap layer that were supplied from Superpower, Inc. After deposition, samples were *in situ* annealed at T_s =773 K and $P(O_2)$=500 Torr, and *ex situ* annealed at 773 K for 1 h in flowing O_2 gas after depositing sputtered Ag electrodes onto the films. The 5-mm-wide × 2-cm-long sample was patterned into a 0.2-mm-wide bridge by laser scribing due to the limits on the maximum measuring current in the characterization system. The standard four-point probe method was used for the transport measurements including superconducting transition temperature T_c and critical current density, J_c, with a voltage criterion of 1 μV/cm. Transmission electron microscopy (TEM) and x-ray diffraction (XRD) were used for microstructural analysis.

The θ-2θ x-ray scans for YBCO films with and without 4 vol % BRETO additions with different RE of Yb, Er, and Gd are shown in Fig. 1(a). All films have sharp out-of-plane *c*-axis orientation with strong (00*l*) peak intensities of YBCO phase. The samples with BRETO additions also have the additional peak at 43 ~ 43.5° corresponding to BRETO(400) which clearly indicates the formation of an oriented BRETO phase within the YBCO film. Since Y^{3+} and RE^{3+} ions have similar ionic radius and same valence, they can be easily substituted with each other and as a result, RE doped YBCO, (Y,*RE*)BCO, and Y doped BRETO, $Ba_2(Y,RE)TaO_6$, are actually formed. Based on detailed XRD analysis involving

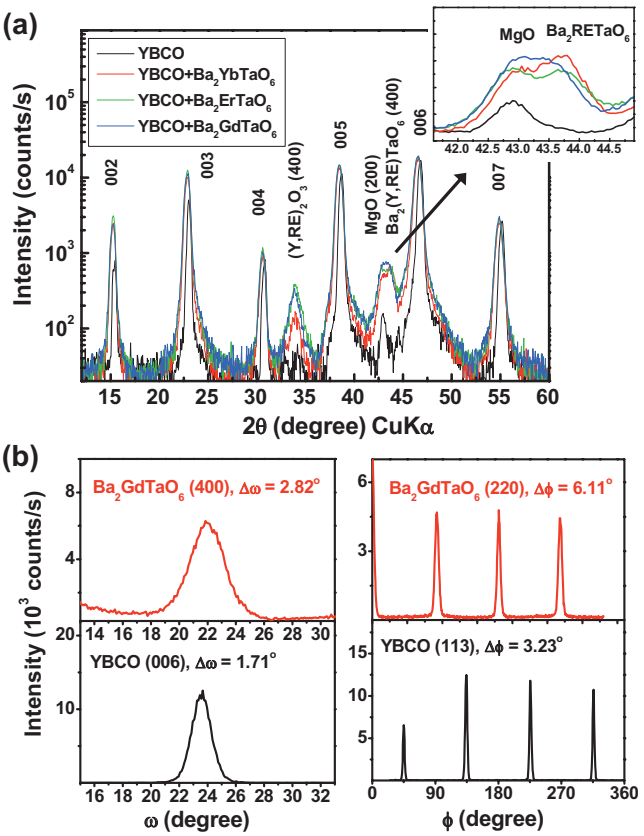

FIG. 1. (Color) X-ray diffraction results for YBCO films with Ba_2RETaO_6 addition. (a) θ-2θ scans for YBCO films with and without 4 vol % Ba_2RETaO_6 addition with *RE* of Yb, Er, and Gd. (b) In-plane and out-of plane textures of (Y,Gd)BCO and $Ba_2(Y,Gd)TaO_6$ phases taken from 4 vol % Ba_2GdTaO_6 doped YBCO film.

peak broadening, the BRETO(400) peak is determined to come from a nanophase with a particle size ~6 nm. The inset of the figure shows the narrow scans for $Ba_2(Y,RE)TaO_6$ peaks measured at the maximum x-ray power. Even though the MgO(200) peak caused by epitaxial MgO layer consisting of IBAD template slightly overlaps with the $Ba_2(Y,RE)TaO_6$ peak, both peaks were clearly distinguishable. It is also observed that the $Ba_2(Y,RE)TaO_6$ peak is shifted to lower angles due to larger lattice parameter with increasing RE^{3+} ionic radius from Yb^{3+} (0.87 Å) to Gd^{3+} (0.94 Å). Strong $Ba_2(Y,RE)TaO_6$ (220) peaks (which have no overlap with peaks for other phases) were observed in θ-2θ scans taken at rotated χ angle of 45° (not shown here). In addition, small peaks at ~34° related to $(Y,RE)_2O_3$ (400) were also detected from the samples with BRETO additions, indicating the presence of small fraction of epitaxial $(Y,RE)_2O_3$ nanoparticles which have a cubic fluorite structure. They were expected due to the slightly off-stoichiometric composition of the YBCO+BRETO targets that were used, i.e., a little excess RE_2O_3 was incorporated in the targets. XRD volume fractions of these $(Y,RE)_2O_3$ particles were measured to be less than 1%. Due to the small quantity, their effect on flux pinning is expected to be also negligible. Figure 1(b) reports omega and phi scans for the (Y,Gd)BCO and $Ba_2(Y,Gd)TaO_6$ phases for the sample with 4 vol % Ba_2GdTaO_6 (BGdTO) addition. Essentially identical omega and phi scans were obtained from films with 4 vol % BRETO with other additions (*RE*=Yb and Er). The x-ray results indicate that $Ba_2(Y,Gd)TaO_6$ nanophase grew in cube-on-cube epitaxial relationship with (Y,Gd)BCO matrix with $[00l]_{BYGdTO}//[001]_{YGdBCO}$. Compared to (Y,Gd)BCO, much larger full-width-half-maximum of omega and phi scans ($\Delta\omega$ and $\Delta\varphi$) for $Ba_2(Y,Gd)TaO_6$ are probably due to some deviation of their alignments with respect to the *c* axis of YBCO.

Cross section TEM examination of the 4 vol % BGdTO-doped YBCO film confirmed the presence of a nanophase with the morphology of nanocolumns of self-assembled $Ba_2(Y,Gd)TaO_6$ nanodots within the (Y,Gd)BCO matrix. As shown in Fig. 2(a), the nanocolumns are, in general, aligned to the crystallographic *c* axis of YBCO but have a splay with some misalignments with respect to the *c* axis of YBCO. Splayed columnar defects are desirable for flux pinning over larger angular regime as already demonstrated in REBCO films with splayed BZO nanocolumns.[10,16] The areal density and cross section of $Ba_2(Y,Gd)TaO_6$ columns was determined via plan-view TEM examination of the film shown in Fig. 2(b). The nanodots have an average diameter of 6–7 nm which is consistent with the estimation by XRD and are separated by a distance of 15–20 nm from each other. The matching field, $B_\phi=\phi_0/a^2$, is calculated to be 5–10 T, where $\phi_0=2.07\times10^{-11}$ T cm^2 is the flux quantum and *a* is the average intercolumn spacing. Selected area diffraction (SAD) pattern in Fig. 2(c) also shows separate and distinguishable diffraction spots caused by $Ba_2(Y,Gd)TaO_6$ cubic, double perovskite structure in addition to those for YBCO.

Excellent superconducting properties are achieved for YBCO films with such BRETO nanocolumns. These films have no T_c reduction over undoped films, implying no poisoning effect due to excellent chemical inertness of BRETO phases with YBCO. The samples with BGdTO addition from 1 up to 4 vol %, have a T_c of 87.4–88.3 K compared to T_c of 87.6 K for pure YBCO. This is in contrast to BZO nanocolumn incorporation which reduces T_c linearly with BZO vol %.[7,13] For instance, a 4 vol % BZO nanocolumn incorporated film has a T_c of ~85 K. Self-field J_c is also improved by BGdTO addition. YBCO+4 vol % BGdTO film was measured to have a J_c of 3.8 MA/cm^2, which is much improved than the J_c of 2.8 MA/cm^2 for pure YBCO. In field J_c performance over entire field and angular ranges is also improved remarkably by the BGdTO nanocolumns as shown in Fig. 3. Field dependent J_c for $H\|c$ in Fig. 3(a) show that BGdTO doped sample has the 1.5–6 fold higher J_c from low up to high magnetic fields compared to pure YBCO film, indicating massive enhancement in flux pinning of YBCO film via self-aligned $Ba_2(Y,Gd)TaO_6$ columns. The irreversibility field, H_{irr} at 77 K is also greatly improved from ~6.3 T to over 8 T (the highest field at which measurements were made) via BGdTO addition. As shown in Fig. 3(b), angular dependence of J_c at 77 K, 1 T and 65 K, 3 T also clearly show twofold to threefold improvement in J_c over entire angular range by incorporation of self-assembled $Ba_2(Y,Gd)TaO_6$ nanocolumns. Even though only a preliminary study has been performed thus far and the doping level

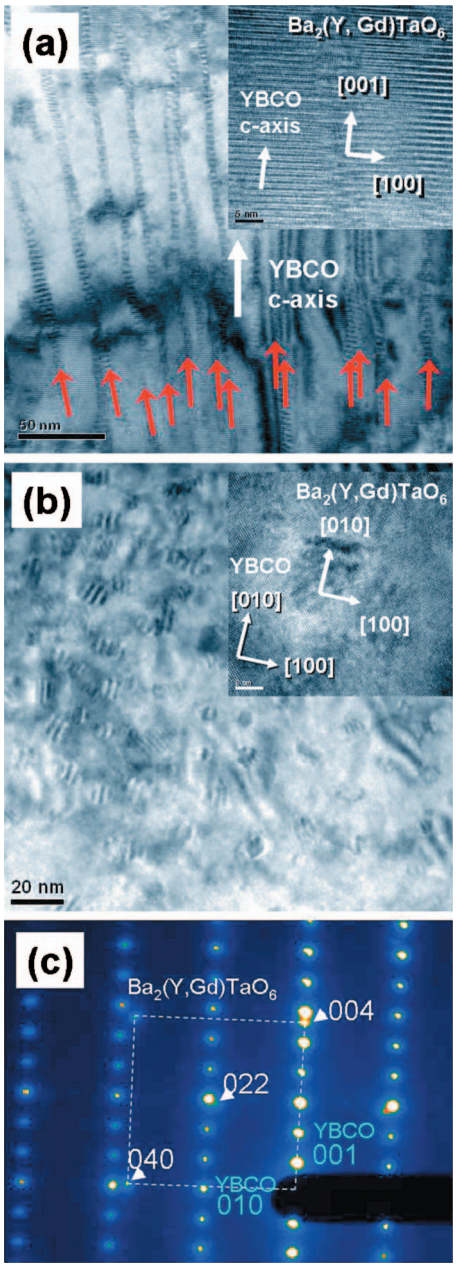

FIG. 2. (Color) Transmission electron micrographs of 0.8-μm-thick YBCO film with 4 vol % Ba_2GdTaO_6 addition on IBAD-MgO templates. (a) Cross-section TEM image showing the presence of splayed columnar defects comprised of self-assembled $Ba_2(Y,Gd)TaO_6$ nanodots in general along the c axis. Inset of the figure is a higher magnification image showing a $Ba_2(Y,Gd)TaO_6$ column. (b) Plan-view TEM image showing distribution of high density of $Ba_2(Y,Gd)TaO_6$ nanocolumns with an average diameter of 6–7 nm and a distance of 15–20 nm separation from each other. Inset of the figure is a higher magnification image showing a $Ba_2(Y,Gd)TaO_6$ nanoparticle. (c) SAD patterns taken from a cross-section TEM specimen indicating the presence of cubic, double perovskite $Ba_2(Y,Gd)TaO_6$ nanocolumns.

and other process conditions still need to be optimized, remarkable improvement in J_c were observed. The improved field and angular dependent J_c for the BGTO-doped sample are similar to the best J_c data obtained on BZO-doped films

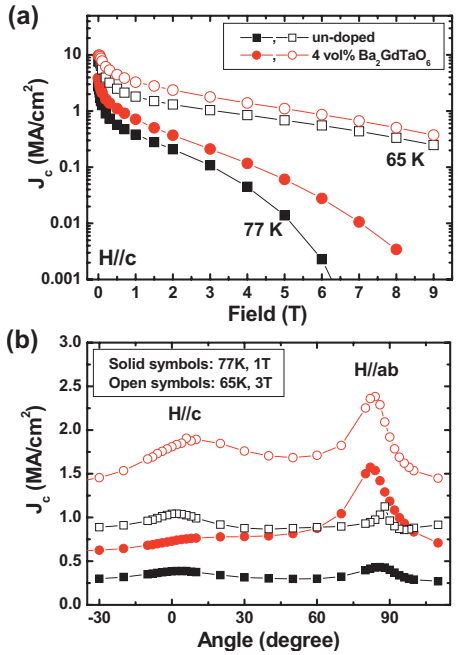

FIG. 3. (Color) The field-dependent J_c at 77 and 65 K for $H\|c$ with the magnetic field up to 8 T (a), and the angular dependent J_c at 77 K, 1 T and 65 K, and 3 T (b) for YBCO and YBCO +4 vol % BGdTO films. All samples have identical film thickness which is 0.8 μm.

which have been optimized over many years of research.[13] In addition, it is expected that compared to BZO, BRETO could form columnar defects more easily over wider processing windows because their larger lattice mismatch of 9–12 % with YBCO would provide a greater driving force for self-assembly of nanodots.

Recently, the compounds with either similar composition or structure to BRETO materials have been reported as possible pinning additives to enhance flux pinning. Rare-earth tantalates, RE_3TaO_7, with pyrochlore phase were reported to form self-assembled nanocolumns and result in enhancement in flux pinning and J_c for YBCO films.[17] However, it is in question that their small lattice mismatches with YBCO less than 4% can produce enough strain leading to self-assembly of nanocolumns composed of RE_3TaO_7 nanodots, when considering our study demonstrating that the high lattice mismatch in the range of 5–12 % is needed for self-assembly.[13] On the other hand, formation of columnar defects comprised of Er-substituted $BaNbO_3$ cubic perovskite, which has a similar lattice constant with $Ba(Er_{0.5}Nb_{0.5})O_6$ phase has been reported from $ErBa_2Cu_3O_x$ with $BaNb_2O_6$ addition.[18] However, the performance of the superconducting film was poor with the maximum self-field J_c of such doped films being 0.2–0.5 MA/cm^2 at 77 K, self-field.

In conclusion, rare-earth barium tantalates having an ordered, double perovskite structure are suggested as promising pinning additives with potentially better pinning over BZO. The c-axis-oriented nanocolumns comprised of self-assembled epitaxial BRETO nanodots with average diameter of 6–7 nm were incorporated into epitaxial YBCO films grown on a biaxially textured coated conductor. No T_c reduction was observed in the compositional range studied (up to

4 vol % BGdTO additions). YBCO films with 4 vol % BGdTO addition exhibited remarkable improvement in flux-pinning and consequently J_c in entire field and angular ranges which are generally 1.5–6 folds as high as J_c for pure YBCO film.

We would like to thank Cliffard C. Davisson for preparing the YBCO+Ba_2RETaO_6 targets by powder mixing, compaction, and sintering. A. Goyal would like to thank SuperPower Inc. for providing the Hastelloy substrates with the multilayer configuration of IBAD MgO layer/Homoepitaxial MgO layer/Epitaxial $LaMnO_3$. This research was sponsored by the U.S. DOE Office of Electricity Delivery and Energy Reliability—Advanced Cables and Conductors under Contract No. DE-AC05-00OR22725 with UT-Battelle, LLC managing contractor for Oak Ridge National Laboratory.

[1] *Second Generation HTS Conductors*, edited by A. Goyal (Kluwer Academic, Boston, MA, 2005).
[2] T. Haugan, P. N. Barnes, R. Wheeler, F. Meisenkothen, and M. Sumption, Nature (London) **430**, 867 (2004).
[3] K. Matsumoto, T. Horide, A. Ichinose, S. Horii, Y. Yoshida, and M. Mukaida, Jpn. J. Appl. Phys., Part 2 **44**, L246 (2005).
[4] J. L. Macmanus-Driscoll, S. R. Foltyn, Q. X. Jia, H. Wang, A. Serquis, L. Civale, B. Maiorov, M. E. Hawley, M. P. Maley, and D. E. Peterson, Nature Mater. **3**, 439 (2004).
[5] J. Gutierrez, A. Llordes, J. Gazquez, M. Gibert, N. Roma, S. Ricart, A. Pomar, F. Sandiumenge, N. Mestres, T. Puig, and X. Obradors, Nature Mater. **6**, 367 (2007).
[6] X. Song, Z. Chen, S. I. Kim, D. M. Feldmann, and D. Larbalestier, Appl. Phys. Lett. **88**, 212508 (2006).
[7] A. Goyal, S. Kang, K. J. Leonard, P. M. Martin, A. A. Gapud, M. Varela, M. Paranthaman, A. O. Ijaduola, E. D. Specht, J. R. Thomson, D. K. Christen, S. J. Pennycook, and F. A. List, Supercond. Sci. Technol. **18**, 1533 (2005).
[8] S. Kang, A. Goyal, J. Li, A. A. Gapud, P. M. Martin, L. Heatherly, J. R. Thompson, D. K. Christen, F. A. List, M. Paranthaman, and D. F. Lee, Science **311**, 1911 (2006).
[9] S. H. Wee, A. Goyal, P. M. Martin, M. Paranthaman, and L. Heatherly, Supercond. Sci. Technol. **19**, L42 (2006).
[10] S. H. Wee, A. Goyal, Y. L. Zuev, and C. Cantoni, Supercond. Sci. Technol. **21**, 092001 (2008).
[11] C. V. Varanasi, P. N. Barnes, J. Burke, L. Brunke, I. Maartense, T. J. Haugan, E. A. Stinzianni, K. A. Dunn, and P. Haldar, Supercond. Sci. Technol. **19**, L37 (2006).
[12] S. H. Wee, A. Goyal, Y. L. Zuev, and C. Cantoni, Appl. Phys. Express **1**, 111702 (2008).
[13] Unpublished.
[14] Y. Doi and Y. Hinatsu, J. Phys.: Condens. Matter **13**, 4191 (2001).
[15] T. G. N. Babu and J. Koshy, J. Solid State Chem. **126**, 202 (1996).
[16] T. Hwa, P. L. Doussal, D. R. Nelson, and V. M. Vinokur, Phys. Rev. Lett. **71**, 3545 (1993).
[17] S. A. Harrington, J. H. Durrell, B. Maiorov, H. Wang, S. C. Wimbush, A. Kursumovic, J. H. Lee, and J. L. MacManus-Driscoll, Supercond. Sci. Technol. **22**, 022001 (2009).
[18] H. Kai, M. Mukaida, R. Teranishi, N. Mori, K. Yamada, S. Horii, A. Ichinose, R. Kita, K. Matsumoto, Y. Yoshida, S. Awaji, K. Watanabe, and T. Fujiyoshi, Physica C **468**, 1854 (2008).